Inorg. Chem. **2007**, *46*, 7840–7847

Modulating Electronic Coupling Using O- and S-donor Linkers

F. Albert Cotton,[†,‡] Zhong Li,[†] Chun Y. Liu,*[,†,§] and Carlos A. Murillo*[,†]

Department of Chemistry and Laboratory for Molecular Structure and Bonding, P.O. Box 3012, Texas A&M University, College Station, Texas 77842-3012, and Department of Chemistry, Tongji University, Shanghai 200092, P. R. China

Received May 14, 2007

Structures of compounds having two dimolybdenum units $Mo_2(DAniF)_3^+$ (DAniF = *N*,*N*′-di-*p*-anisylformamidinate) connected by unsubstituted oxamidate (**1**) and dithiooxamidate (**2**) linkers are isomorphous, and the cores of the molecules are planar because of two intramolecular hydrogen bonds within the linkers. Molecular mechanics calculations show a barrier of rotation along the C–C bond of ∼10 kcal·mol^{-1}, which suggests that planar conformations are also expected in solution. Changing the two oxygen atoms in the linker of **1** to sulfur atoms results in a significant enhancement of the electronic coupling between the dimetal units ($\Delta E_{1/2}$ = 204 mV for **1** and 407 mV for **2**). The electronic spectrum of **2** shows an intense low energy (600 nm) metal-to-ligand charge transfer (MLCT) band, whereas that for **1** shows only a weak absorption band at 460 nm. DFT calculations on models **1′** and **2′**, in which the anisyl groups were replaced by hydrogen atoms, show that the energy of the π^* orbital of the linker is much lower for **2′**. This allows dπ–dδ interactions from the electrons in the δ orbitals of the Mo_2 unit to the sulfur atom that in turn facilitates an electron hopping pathway.

Introduction

Intramolecular electron transfer between a donor and an acceptor group is a fundamental process in chemistry, biology, physics, and also in molecular electronics.[1] Extensive studies on compounds with redox units, mainly single metal units, bridged by conjugated electron carriers, such as polyenes and polypyrroles, have provided insight into electronic coupling processes and electron-transfer mechanisms.[2] Recently, dimetal units with multiple metal−metal bonds have been employed to study electronic communication through a variety of linkers and show attractive features because their well-known structural and spectroscopic properties may serve as probes to follow these processes.[3] In general, these complexes may be expected to be useful as molecular wires or single-molecule transistors.[4]

Dicarboxylate groups have been the most common linkers for bridging two dimetal units, but such groups generally lead to weak electronic coupling. Moreover, it has been shown that in *dimers of dimers* of the type $[(DAniF)_3Mo_2]_2$-$(\mu-O_2C(CH{=}CH)_nCO_2]$, where n = 0−4 and DAniF = *N*,*N*′-di-*p*-anisylformamidinate, electronic communication between the two quadruply bonded $[Mo_2]$ units diminishes as the separation between them increases.[5] The oxalate-linked analogue affords the strongest coupling for all of the known species with dicarboxylate linkers, with $\Delta E_{1/2}$ = 212 mV,[5]

* To whom correspondence should be addressed. E-mail: cyliu06@mail.tongji.edu.cn (C.Y.L), murillo@tamu.edu (C.A.M.).
† Texas A&M University.
‡ Deceased February 20, 2007.
§ Tongji University.

(1) See for example: (a) Lin, J. P.; Balabin, I. A.; Beratan, D. N. *Science*, **2005**, *310*, 1311. (b) Li, N.; Xu, J. Z.; Yao, H.; Zhu, J. J.; Chen, H. Y. *J. Phys. Chem. B*, **2006**, *110*, 11561. (c) Gray, H. B.; Winkler, J. R. *Q. Rev. Biophys.* **2003**, *36*, 341. (d) Tan, M. L.; Balabin, I.; Onuchic, J. N. *Biophys. J.* **2004**, *86*, 1813.
(2) See for example: (a) Tolbert, L. M.; Zhao, X.; Ding, Y.; Bottomley, L. A. *J. Am. Chem. Soc.* **1995**, *117*, 12891. (b) Ribou, A.-C.; Launay, J.-P.; Sachtleben, M. L.; Li. H.; Spangler, C. W. *Inorg. Chem.* **1996**, *35*, 3735. (c) Sutter, J. P.; Grove, D. M.; Beley, M.; Collin, J. P.; Veldman, N.; Spek, A. L.; Sauvage, J. P.; Koten, G. V. *Angew. Chem., Int. Ed. Engl.* **1994**, *33*, 1282.
(3) See for example: (a) Chisholm, M. H.; Macintosh, A. M. *Chem. Rev.* **2005**, *105*, 2949. (b) Cotton, F. A.; Lin, C.; Murillo, C. A. *Acc. Chem. Res.* **2001**, *34*, 759. (c) Xu, G. L.; Zou, G.; Ni, Y. H.; DeRosa, M. C.; Crutchley, R. J.; Ren, T. *J. Am. Chem. Soc.* **2003**, *125*, 10057. (d) Miyasaka, H.; Campos-Fernández, C. S.; Galán-Mascarós, J. R.; Dunbar, K. R. *Inorg. Chem.* **2000**, *39*, 5870. (e) Bursten, B. E.; Chisholm, M. H.; Clark, R. J. H.; Firth, S.; Hadad, C. M.; Wilson, P. J.; Woodward, P. M.; Zaleski, J. M. *J. Am. Chem. Soc.* **2002**, *124*, 12244. (f) Cotton, F. A.; Lin, C.; Murillo, C. A. *Proc. Natl. Acad. Sci. U.S.A.* **2002**, *99*, 4810.
(4) (a) Launay, J.-P. *Chem. Soc. Rev.* **2001**, *30*, 386. (b) Basch, H.; Ratner, M. A. *J. Chem. Phys.* **2005**, *123*, 234704.
(5) (a) Cotton, F. A.; Donahue, J. P.; Murillo, C. A.; Pérez, L. M. *J. Am. Chem. Soc.* **2003**, *125*, 5486. (b) Cotton, F. A.; Donahue, J. P.; Murillo, C. A. *J. Am. Chem. Soc.* **2003**, *125*, 5436. (c) Cotton, F. A.; Donahue, J. P.; Lin, C.; Murillo, C. A. *Inorg. Chem.* **2003**, *40*, 1234.

10.1021/ic700932s CCC: $37.00
Published on Web 08/17/2007

Scheme 1

Scheme 2

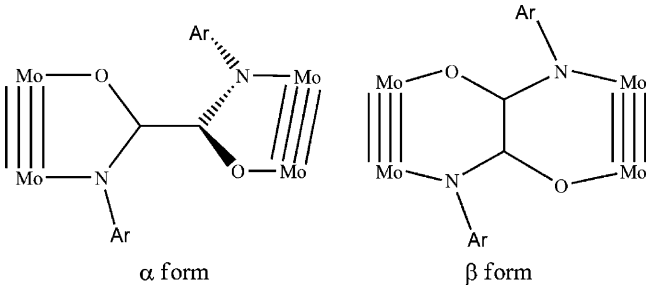

which corresponds to a comproportionation constant, K_c, of 3.8×10^3.[6] In the solid state, the $[Mo_2](O_2C-CO_2)[Mo_2]$ core is flat and has an ideal D_{2h} geometry in which the two Mo_2 units are essentially parallel (Scheme 1).[5] However, it has been noted[7] that free rotation along the C−C single bond is possible in solution. Chisholm and co-workers have suggested that the free rotation in solution may be inhibited in dicarboxylate-linked compounds, by using functionalized terephthalate linkers.[8] Changes in the electronic spectra were offered as indicators of the effect of metal-to-ligand back-bonding, upon changes in the dihedral angle between the C_6 ring and the CO_2 units. But, how the parallel (flat core) and perpendicular conformations (Scheme 1) affect the electrochemical behavior and thus the electronic communication remained unclear.

It should be noted that when dioxamidate dianions −RN(O)C−C(O)NR− (R = C_6H_5 or *p*-$CH_3OC_6H_4$) were used to link $[Mo_2]$ units instead of dicarboxylate groups, two isomers (Scheme 2) with distinct electronic communication formed.[9] In the α isomers, the diamidate linkers were nonplanar, with the two $[Mo_2]$RN(O)C planes being approximately perpendicular to each other as a result of steric repulsion from the bulky R groups, whereas the *β* isomers have heteronaphthalene−like structures.[10] The electrochemistry for the α compounds show $\Delta E_{1/2}$ values of about 190 mV that correspond to K_c values of about 1.7×10^3. Interestingly, these values resemble those in the oxalate analogue.

In this work, we used the unsubstituted oxamidate dianion, −HN(O)C−C(O)NH−, to bridge two $[Mo_2]$ units and also the sulfur analogue (dithiooxamidate −HN(S)C−C(S)NH−)

Scheme 3

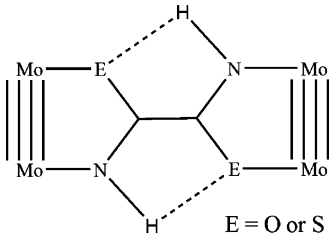

to probe the differences in electronic communication. Interest in the use of sulfur compounds developed from the fact that many molybdenum enzymes contain terminal sulfur donor ligands.[11] These sulfur atoms appear to be crucial to enzyme reactivity, particularly because of the possibility that Mo−S orbital overlap may provide an effective low-energy pathway for electron transfer to and from the metal.[12,13] However, electronic communication through S-donor ligands has been scantly studied.

We report that the presence of EC−CNH groups (E = O, S), intramolecular hydrogen-bonding interactions stabilize planar conformations in the *dimers of dimers* (Scheme 3) and thus differ from the perpendicular arrangement found in the α isomers in Scheme 2. Electronic coupling between dimetal centers in $[Mo_2]L[Mo_2]$ compounds (L = oxamidate) was greatly enhanced by changing the oxygen atoms in the linker to sulfur atoms.

Results and Discussion

Syntheses and Structural Results. Previously, we have reported the syntheses of α or *β* isomers (Scheme 2) of *dimers of dimers* having $[Mo_2]$ units linked by aryl-substituted oxamidate ligands.[9] Here, the unsubstituted oxamidate linker (−HN(O)C−C(O)NH−) is used to explore (1) the effect of diminishing steric crowding by removing aryl groups on the nitrogen atoms and (2) the possibility of forming intramolecular hydrogen bonds that may favor a planar core. The reactions, summarized by the equations below, gave a yellow precipitate for the dioxamidate and a blue solution for the dithioxamidate, **1** and **2**, respectively.[14] The products were shown by ^{1}H NMR spectroscopy to consist of only one species.

(6) The K_c is related to the $\Delta E_{1/2}$ value (in mV) by the relationship: $K_c = 10^{\Delta E/59}$. See for example: (a) Ketterle, M.; Fiedler, J.; Kaim, W. *Chem. Commun*. **1998**, 1701. (b) Demadis, K. D.; Hartshorn, C. M.; Meyer, T. *Chem. Rev.* **2001**, *101*, 2655.

(7) Bursten, B. E.; Chisholm, M. H.; Clark, R. J. H.; Firth, S.; Hadad, C. M.; Macintosh, A. M.; Wilson, P. J.; Woodward, P. M.; Zaleski, J. M. *J. Am. Chem. Soc.* **2002**, *124*, 3050.

(8) Chisholm, M. H.; Feil, F.; Hadad, C. M.; Patmore, N. J. *J. Am. Chem. Soc.* **2005**, *127*, 18150.

(9) (a) Cotton, F. A.; Liu, C. Y.; Murillo, C. A.; Villagrán, D.; Wang, X. *J. Am. Chem. Soc.* **2003**, *125*, 13564. (b) Cotton, F. A.; Liu, C. Y.; Murillo, C. A.; Zhao, Q. *Inorg. Chem.* **2007**, *46*, 2604.

(10) Cotton, F. A.; Liu, C. Y.; Murillo, C. A.; Villagrán, D.; Wang, X. *J. Am. Chem. Soc.* **2004**, *126*, 14822.

(11) (a) Hille, R. *Chem. Rev.* **1996**, *96*, 2757. (b) Czjzek, M.; Santos, J.-P. D.; Pomier, J.; Giordano, G.; Méjean, V.; Haser, R. *J. Mol. Biol.* **1998**, *284*, 435. (c) Hänzelmann, P.; Schindelin, H. *Proc. Natl. Acad. Sci. U.S.A.* **2004**, *101*, 12870. (c) Brondino, C. D.; Rivas, M. G.; Romao, M. J.; Moura, J. J. G.; Moura, I. *Acc. Chem. Res.* **2006**, *39*, 788.

(12) (a) Enemark, J. H.; Cooney, J. J. A.; Wang. J.-J.; Holm, R. H. *Chem. Rev.* **2004**, *104*, 1175. (b) Carducci, M. D.; Brown, C.; Solomon, E. I.; Enemark, J. H. *J. Am. Chem. Soc.* **1994**, *116*, 11856.

(13) It should be noted that for third period elements such as silicon, phosphorus, and sulfur, the low-lying 3d orbitals can be utilized not only for pπ−dπ multiple bonding but also for additional bond formation. See for example: Cotton, F. A.; Wilkinson, G.; Gaus, P. L. *Basic Inorganic Chemistry*, 3rd ed.; John Wiley & Sons, Inc.: New York, 1995; pp 258−259.

(14) Efforts to isolate the mixed-valence species using 1 equiv of the oxidizing agents $Cp_2Fe_2PF_6$ or $AgPF_6$ have been unsuccessful. After the addition of the oxidizing agents to the neutral compounds in CH_2Cl_2 at −78 °C followed by warming to room temperature, the color of **1** changed from yellowish to brown, but no identifiable product was obtained. No significant color change was observed for **2**. This is common for most compounds of this type as only a few *dimers of dimers* having mixed-valence species have been isolated and characterized.

$$Mo_2(DAniF)_3(O_2CCH_3) + NaOCH_3 \xrightarrow{THF} Mo_2(DAniF)_3(OCH_3)(HOCH_3) + NaO_2CCH_3$$

$$2Mo_2(DAniF)_3(OCH_3)(HOCH_3) + H_2N(E)CC(E)NH_2 \rightarrow [Mo_2(DAniF)_3]_2[HN(E)CC(E)NH] + 2CH_3OH$$

E = O or S

Compound **1** crystallized in space group $P\bar{1}$, with the molecule residing on an inversion center. To a first approximation, the core (Figure 1) resembles that of the α isomers in that the C−$C_{oxamidate}$ bond is perpendicular to the Mo−Mo bonds. However, closer inspection shows a major difference with the α isomers in that the two Mo_2 units are parallel to each other as in the *β* isomers. Because of two intramolecular O···H−N hydrogen bonds, the core in **1** is planar and the core of the molecule has idealized C_{2h} symmetry. Its structure is thus a hybrid between that of the α and *β* forms. The distance from the crystallographically independent oxygen to the amino hydrogen atom is ca. 2.41 Å. These two hydrogen bonds stabilize the planar conformation of **1**. Molecular mechanics calculations on these two compounds (vide infra) show that the energy for the planar conformation is about 10 kcal/mol lower than the conformation in which the Mo_2 units are essentially perpendicular. This results in a high barrier of rotation along the C−C bond and suggests that the core should be locked in this planar conformation even in solution.

The Mo−Mo distance of 2.0907(8) Å (Table 1) is typical of quadruply bonded compounds having dimolybdenum species embraced by four, three-atom bridging ligands, such as $Mo_2(DAniF)_4$[15] and $Mo_2(OCCH_3)_4$.[16] For comparison, the Mo−Mo distances for α or *β* forms linked by *N*,*N*′-di-*p*-anisyloxamidate are 2.0927(8) and 2.0944(4) Å.[9] The distance between the midpoints of the two Mo−Mo units is 6.978 Å, close to the values in the α form.[9] The bond distance in the central C−C unit (1.51(1) Å) is similar to that in oxalic acid and corresponds to a carbon−carbon single bond.[17]

The analogous ligand containing two S donor atoms, dithiooxamidate, was used as a linker in **2**. This compound was synthesized similarly to **1** but it is much more soluble in THF and dichloromethane than **1**. Crystals of the two compounds are isomorphous, having similar cell dimensions and four interstitial CH_2Cl_2 molecules per formula unit. The molecule, whose core is shown in Figure 1, resides on an inversion center, and it has a Mo−Mo bond distance of 2.0895(10) Å that resembles that in **1**. The major contrast between these molecules derives from the difference in M−E distances. Because the Mo−S distance (2.462(3) Å) is about 0.33 Å longer than the Mo−O distance, the nonbonding separation between the two Mo_2 units measured by the midpoints of the Mo_2 axis increases by about 0.5 Å from 6.978 to 7.471 Å. The change in the Mo−E distances also results in the different angles of the five-membered ring that is defined by the [Mo_2] unit and the CNE group (Table 1). All of the other distances and angles are as expected.

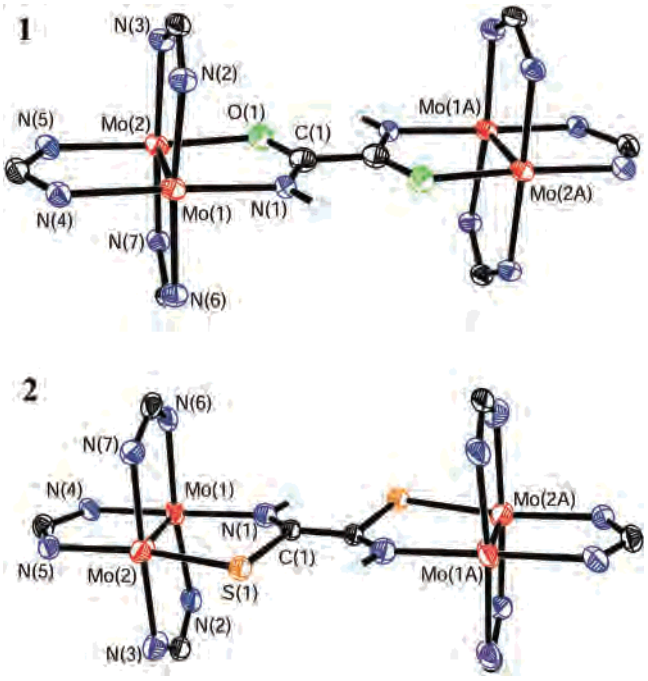

Figure 1. Core structures of **1** and **2** with displacement ellipsoids drawn at the 40% probability level. All of the *p*-anisyl groups and most of the hydrogen atoms have been omitted for clarity.

Table 1. Selected Bond Lengths (Angstroms) and Angles (Degrees) for **1** and **2**

	1·4CH_2Cl_2	**2**·4CH_2Cl_2
Mo(1)−Mo(2)	2.0907(8)	2.0895(13)
Mo(2)−O(1)	2.134(3)	
Mo(2)−S(1)		2.462(3)
Mo(1)−N(1)	2.127(3)	2.181(10)
Mo(1)−N(2)	2.160(4)	2.137(6)
Mo(1)−N(4)	2.133(4)	2.156(5)
Mo(1)−N(6)	2.159(4)	2.133(6)
Mo(2)−N(3)	2.141(3)	2.155(6)
Mo(2)−N(5)	2.145(4)	2.136(5)
Mo(2)−N(7)	2.129(4)	2.174(6)
C(1)−O(1)	1.320(6)	
C(1)−S(1)		1.67(2),
C(1)−N(1)	1.293(6)	1.31(2)
N(1)−C(1)−O(1)	124.6(4)	
N(1)−C(1)−S(1)		120.9(1)
Mo(1)−N(1)−C(1)	115.1(3)	130.4(10)
Mo(2)−O(1)−C(1)	114.2(3)	
Mo(2)−S(1)−C(1)		97.1(5)

It should be noted that the unsubstituted linkers, −HN(E)C−C(E)NH−, differ in another important aspect with respect to other diamidate and dicarboxylate ligands used thus far to make *dimers of dimers* because they still have two amino hydrogen atoms (N−H), which may be capable of undergoing further deprotonation under appropriate conditions. Indeed, a derivative of the sulfur compound having the formula {[$Mo_2(DAniF)_3$]$_2$(Li_2($THF)_4$(NSC−CNS))}·2THF, **3**·2THF, has been isolated and its structure is provided as Supporting Information.[18]

Electrochemistry. Electrochemistry has been a widely used tool for evaluating electronic communication between redox-active metal centers.[19] For the dimer of dimolybdenum compounds, electrochemistry usually shows two consecutive

(15) Lin, C.; Protasiewics, J. D.; Smith, E. T.; Ren, T. *Inorg. Chem.* **1996**, *35*, 6422.
(16) Cotton, F. A.; Mester, Z. C.; Webb, T. R. *Acta Crystallogr.* **1974**, *B30*, 2768.
(17) Ayerst, E. M.; Duke, J. R. C. *Acta Crystallogr.* **1954**, *7*, 588.

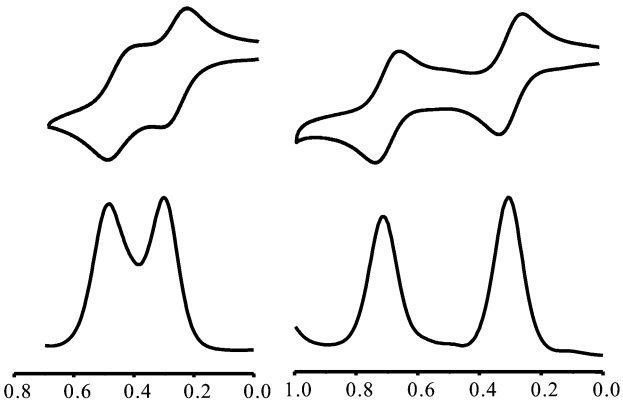

Figure 2. Cyclic voltammograms (with potentials vs Ag/AgCl) and differential pulse voltammograms (DPV) for **1** (left) and **2** (right) in a CH_2Cl_2 solution.

reversible one-electron redox processes, and the separation between these two waves, $\Delta E_{1/2}$, is associated with the comproportionation constant K_c.

$$M_2^{II}\sim M_2^{II} + M_2^{III}\sim M_2^{III} \overset{K_c}{\rightleftharpoons} 2M_2^{III}\sim M_2^{II}$$

The free energy of comproportionation, ΔG_c, is calculated using the relationship $\Delta G_c = -RT\ln(K_c)$. The value of ΔG_c may be viewed as being affected by a series of contributing factors.[20] A commonly used expression is[21]

$$\Delta G_c = \Delta G_s + \Delta G_e + \Delta G_r + \Delta G_i$$

where ΔG_s is a small statistical contribution to the comproportionation equilibrium, ΔG_e accounts for the electrostatic repulsion of the metal centers, ΔG_r is the free energy of resonance exchange or electron delocalization, and ΔG_i is a contribution from inductive factors.

To some extent, K_c values obtained under similar experimental conditions for closely related systems may be used as a measurement for comparing electronic coupling between metal centers through a linker. Previous studies show that the distance between the Mo_2 units and the metal-to-ligand back-bonding plays a significant role in modifying the electronic coupling.[22] The cyclic voltammogram (CV) of **1** shows two reversible oxidation processes (Figure 2), and the potential difference between the two waves, $\Delta E_{1/2}$, is 204 mV ($E_{1/2}(1) = 280$, $E_{1/2}(2) = 484$ mV), corresponding to a comproportionation constant of 2.8×10^3. As shown in Table 2, this number is similar to those for compounds linked by oxalate and substituted oxamidates in the α isomers. The distances between the dimetal units in all of these compounds are essentially the same (ca. 7 Å). However, the relative orientation of $[Mo_2]$ units in solutions is different; planar for **1**, with free rotation along the C−C single bond for the oxalate analogue, and perpendicular for the α form in aryl-substituted oxamidates. This leads to the conclusion that the electronic coupling in these compounds is essentially due to the electrostatic repulsion, with little contribution from electron delocalization due to resonance exchange. For these essentially localized systems, the dihedral angles between the two $[Mo_2]$ units have little influence on the electronic coupling.[23]

The CV of **2** also shows two redox processes with $\Delta E_{1/2}$ of 407 mV ($E_{1/2}(1) = 294$, $E_{1/2}(2) = 701$ mV), which results in a comproportionation constant of 7.6×10^6. Comparison of the electrochemistry for **1** and **2** revealed that the electronic coupling between the metal centers is enhanced by changing the oxygen donor atoms in the oxamidate bridge to sulfur atoms in the dithiooxamidate linkers. Because the two compounds share a common core structure and the distance between the metal centers in **2** is about 0.5 Å longer than in **1**,[24] the enhancement in electronic communication must be attributed to an effect other than electrostatic interactions between metal centers.[25] It appears that the low-energy metal-to-sulfur back-bonding pathway is the main reason for the enhanced electronic communication upon changing oxygen to sulfur atoms, vide infra. Similar effects were observed for the successive substitution of oxygen with sulfur in dicarboxylates for the compounds $[(Bu^tCO_2)_3M_2]_2(X_2CC_6H_4CX_2)$ (M = Mo and W, X = O or S).[26] A summary of electrochemical data for these closely related systems is provided in Table 3.

Electronic Structure and UV−Vis Spectra. Density functional theory (DFT) calculations were performed on the models **1′** and **2′**, which represent **1** and **2** with the anisyl groups in the auxiliary formamidinate groups replaced by hydrogen atoms.

Previous studies on the substituted oxamidate-linked compounds show that both the steric and electronic interactions have influence on the stability of the α isomers.[9] As shown by the structures of **1** and **2**, the cores of the *dimers of dimers* with unsubstituted linkers have a planar conformation due to the hydrogen bonding. This conformation also minimizes steric interactions. The optimized geometries for

(18) The addition of methyllithium to a suspension of **1** in THF at −70 °C did not show any apparent change, but under similar conditions, the color of a solution of **2** immediately changed from dark blue to orange. From such a solution, a lithium salt having the formula $\{[Mo_2(DAniF)_3]_2(Li_2(THF)_4(NSC{-}CNS))\}\cdot 2THF$, **3**·2THF was isolated. See the supporting information.

(19) Richardson, D. E.; Taube, H. *Coord. Chem. Rev.* **1984**, *60*, 107.

(20) See for example: (a) DeRosa, M. C.; White, C.; Evans, C. E. B.; Crutley, R. J. *J. Am. Chem. Soc*. **2001**, *123*, 1396. (b) Chen, Y. J.; Pan, D.-S.; Chiu, C.-F.; Su, J.-X.; Lin, S. J.; Kwan, S. K. *Inorg. Chem*. **2000**, *39*, 953.

(21) Evans, C. E. B.; Naklicki, M. L.; Rezvani, A. R.; White, C. A.; Kondratiev, V. V.; Crutchley, R. J. *J. Am. Chem. Soc.* **1998**, *120*, 13096.

(22) Cotton, F. A.; Murillo, C. A.; Villagrán, D.; Yu, R. *J. Am. Chem. Soc.* **2006**, *128*, 3281.

(23) For the functionalized terephthalate-linked compounds, the electronic spectra changed according to the dihedral angles between the two $[Mo_2]$ axes, but the electrochemistry was not studied. See ref 8.

(24) It should be noted that the electronic coupling between the dimetal centers is not necessarily enhanced if the core structure has a π system or if the conformation is changed by the substitution of oxygen to sulfur atoms.

(25) As it is often recognized (ref 13), an important difference between sulfur and oxygen compounds is that the sulfur d orbitals are available for additional bonding interactions, and sulfur atoms frequently use dπ interactions to form multiple bonds. For example, in the sulfate ion, the S−O bonds have considerable multiple-bond character, as evidenced by the shortness of the bond distance. See: Cotton, F. A.; Wilkinson, G.; Murillo, C. A.; Bochmann, M. *Advanced Inorganic Chemistry*, 6th Ed.; John Wiley & Sons, Inc: New York, 1999.

(26) Chisholm, M. H.; Patmore, N. J. *Dalton Trans.* **2006**, 3164.

Table 2. Comparison of Electrochemical Data for Compounds with Two [Mo_2] Units Linked by Oxalate and Dioxamidate Bridges

linker	orientation of [Mo_2] in solution	[Mo_2]···[Mo_2] (Å)	$E_{1/2}(1)$ (mV)	$E_{1/2}(2)$ (mV)	$\Delta E_{1/2}$ (mV)	K_c	ref
oxalate	free rotation	6.953	294	506	212	3.8×10^3	5
α−diphenyloxamidate	⊥	7.096	176	367	191	1.7×10^3	9a
α−di−*p*−anisyloxamidate	⊥	7.081	183	373	190	1.6×10^3	9a
dioxamidate	||	6.978	280	484	204	2.8×10^3	this work

Table 3. Comparison of Electrochemical Data for Compounds with Two M_2 Units (M = Mo and W) Bridged by Related O- and S-donor Containing Linkers

compound	$E_{1/2}(1)$ (mV)	$E_{1/2}(2)$ (mV)	$\Delta E_{1/2}$ (mV)	K_c	ref
$[(Bu^tCO_2)_3Mo_2]_2(O_2CC_6H_4CO_2)$	0	NA	0	4	30
$[(Bu^tCO_2)_3Mo_2]_2(OSCC_6H_4CSO)$	0	184	184	1.3×10^3	26
$[(Bu^tCO_2)_3W_2]_2(O_2CC_6H_4CO_2)$	−340	−180	160	5.1×10^2	30
$[(Bu^tCO_2)_3W_2]_2(OSCC_6H_4CSO)$	−78	−260	518	5.7×10^8	26
$[Mo_2(DAniF)_3]_2$(oxamidate)	280	484	204	2.8×10^3	this work
$[Mo_2(DAniF)_3]_2$(dithiooxamidate)	294	701	407	7.6×10^6	this work

Table 4. Calculated Energies and Geometries for Models **1′** and **2′**

model	energy	HOMO	HOMO−1	Δ*E*	calculated bond lengths (Å) and angles (deg)				
	(a.u.)	(eV)	(eV)	(eV)	Mo−Mo	Mo_2···Mo_2	$Mo-N_{DAniF}$	$Mo-N_{linker}$	Mo−E
1′	−1504.2992	−3.47	−3.81	0.34	2.139	7.102	2.143	2.151	2.154
2′	−2150.2597	−3.63	−4.08	0.45	2.141	7.609	2.145	2.127	2.550

1′ and **2′** are shown schematically in part (a) of Figure 3 and differ from the geometries of the α isomers (part (b) of Figure 3) in that the former have parallel Mo_2 units, whereas the latter have essentially perpendicular Mo_2 units. However, the optimized geometries in part (a) of Figure 3 are consistent with those in the crystal structures, which also show a planar core.

Vibrational frequency analysis using the optimized models indicated that these geometries represent true minima on the potential energy surfaces. Selected optimized parameters are summarized in Table 4. Although calculated distances are generally longer than those from the crystal structures (Table 1) because of the simplification in replacing the *p*-anisyl groups with less-basic hydrogen atoms, there is consistency between experimental and calculated parameters. For example, the calculated difference in the nonbonding distance between the dimetal units of 0.507 Å (7.471 Å for **1′** and 7.102 Å for **2′**) is in good agreement with that from the crystal structures (0.493 Å).

Molecular orbital analysis from DFT calculations provides valuable information on the electronic structure of the two compounds. For the two models, the HOMO and HOMO−1 are the out-of-phase ($\delta-\delta$) and in-phase ($\delta+\delta$) combinations of the δ orbitals in Mo_2 units (Figure 4), respectively, and they resemble each other. Because to some extent, the splitting of the HOMO and the HOMO−1 is a measure of the electronic coupling between the Mo_2 units; the larger the energy gap between the HOMO and HOMO−1, the stronger the electronic communication (and vice versa). For example, in dimers having dimolybdenum units linked by dioxolene dianions, which have the strongest electronic communication so far reported ($K_c = \sim 10^{12-13}$), the energy difference between HOMO and HOMO−1 is 0.98 eV. This

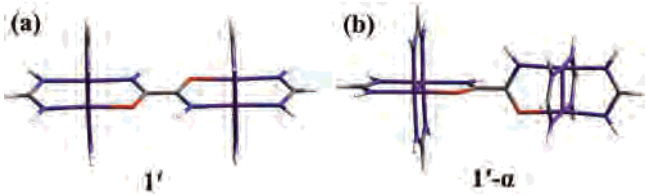

Figure 3. View of the geometry for the optimized geometries having a planar core (a) contrasted with the perpendicular conformations (b) similar to those in the α isomers.

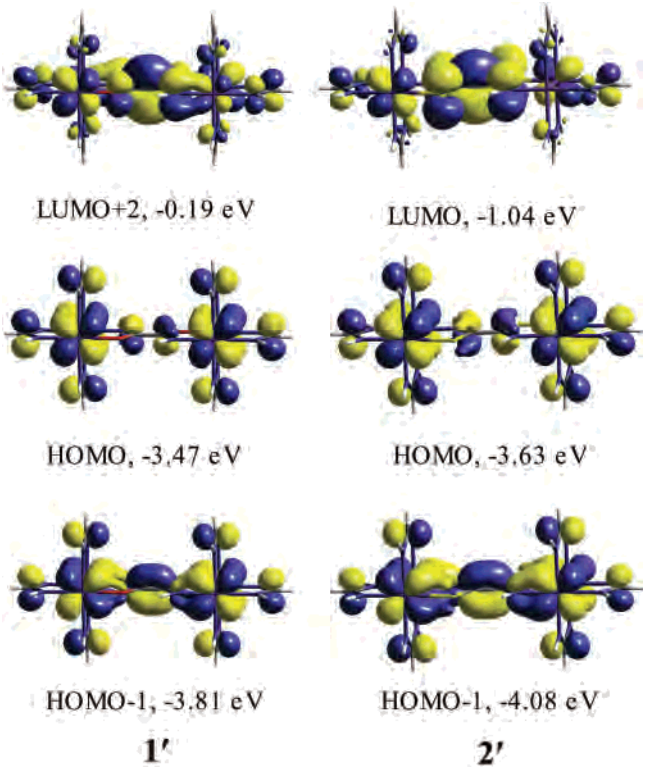

Figure 4. Illustration of the 0.02 contour surface diagrams for selected frontier orbitals for **1′** and **2′**. Note that the HOMO and HOMO−1 for **1′** and **2′** are similar and are in-phase ($\delta+\delta$) and out-of-phase ($\delta-\delta$) combinations of the δ orbitals in Mo_2 units, whereas the linker π^* is LUMO+2 for **1′** and LUMO for **2′**.

Table 5. Calculated Frontier MO Energies for the Models **1′** and **2′**

	$[(HNC(H)NH)_2Mo_2]_2(C_2O_2N_2H_2)$ (**1′**)		$[(HNC(H)NH)_2Mo_2]_2(C_2S_2N_2H_2)$ (**2′**)	
frontier orbitals	MO energy (ev)	assignment	MO energy (ev)	assignment
LUMO+5	0.3034	$Mo_4\ \pi^*+\pi^*$	0.0726	$Mo_4\ \pi^*+\pi^*$
LUMO+4	0.0871	$Mo_4\ \delta^*-\delta^*$	−0.1233	$Mo_4\ \delta^*-\delta^*$
LUMO+3	−0.0220	$Mo_4\ \delta^*+\delta^*$	−0.2857	$Mo_4\ \delta^*+\delta^*$
LUMO+2	−0.1910	Linker π^*	−0.3494	$Mo_4\ \sigma^*-\sigma^*$
LUMO+1	−0.2291	$Mo_4\ \sigma^*-\sigma^*$	−0.3975	$Mo_4\ \sigma^*+\sigma^*$
LUMO	−0.3020	$Mo_4\ \sigma^*+\sigma^*$	−1.0374	Linker π^*
HOMO	−3.4736	$Mo_4\ \delta-\delta$	−3.6344	$Mo_4\ \delta-\delta$
HOMO−1	−3.8129	$Mo_4\ \delta+\delta$	−4.0754	$Mo_4\ \delta+\delta$
HOMO−2	−5.0780	Ligand	−4.8721	Ligand
HOMO−3	−5.0965	Ligand	−5.0408	Ligand
HOMO−4	−5.5294	$Mo_4\ \pi-\pi$	−5.4492	Ligand

is also the largest number obtained from DFT calculations for dimers having Mo_2 units.[22]

For the models **1′** and **2′**, the calculated ΔE values are 0.34 and 0.45 eV, respectively. The larger energy gap between the HOMO and HOMO−1 for model **2′** is consistent with the larger separation observed between redox waves in **2** than in **1**. This is in agreement with the commonly observed increased use of d orbitals for sulfur compounds, such as in $d\pi-p\pi$ and $d\pi-d\pi$ interactions,[25] and also with what was found for $[(HCO_2)_3Mo]_2(E_2CC_6H_4CE_2)$ model compounds (E = O or S), in which the energy of the HOMO decreased from −3.47 eV for the model having E = oxygen to −3.63 eV for the model with E = sulfur.[26] In all of these compounds, there are π antibonding interactions between the linker π orbitals and the Mo_2 δ combination in the HOMO. Because the $d\pi$ orbitals of the sulfur atoms in the linkers accept electrons from the δ orbitals of the dimetal units, there is an electron pathway that has some $d\pi-d\delta$ character.[27] Chisholm and Patmore have also suggested that the π donation of the sulfur 3p orbital is less than that of the oxygen 2p orbital, which accounts for the downward trend in energy of the HOMO.[26]

Although the HOMO and HOMO−1 for models **1′** and **2′** are similar in shape, there are substantial differences in their electronic structures. Selected energies of frontier MOs of models **1′** and **2′** along with the main contributions are in Table 5. It is important to compare the energies of the linker π^* orbitals for **1′** and **2′**, which are −0.19 eV for the LUMO+2 and −1.04 eV for the LUMO, respectively. Two mechanisms for the electronic communication, electron hopping and hole hopping (Scheme 4) have been proposed for the *dimers of dimers*.[28] A comparison of the energy of the linker π^* and π orbitals relative to those of the Mo_2 δ combinations is considered critical in electron-hopping and hole-hopping pathways. For **1′** and **2′**, the linker π-orbital energies are far below the HOMO−1, and hole hopping is expected to contribute very little to the electronic coupling. The energy difference between the HOMO and linker π^* orbital are 3.28 and 2.59 eV for **1′** and **2′**, respectively. Therefore, the enhanced electronic coupling between dimetal centers when sulfur atoms are used in the linker instead of oxygen atoms is proposed to be caused by the low-energy metal-to-sulfur pathway.

The smaller energy gap between Mo_2 δ orbitals and the linker π^* orbitals in **2′** is consistent with the electronic spectra. The UV−vis spectrum of **1** shows two absorption bands at 412 and 460 nm (Figure 5). From time-dependent density functional (TD−DFT) calculations, the absorption at 412 nm can be assigned to $\delta \rightarrow \delta^*$ transitions, which rises from a transition from the HOMO-1 to the LUMO+3 ($\delta+\delta \rightarrow \delta^*+\delta^*$) and from the HOMO to the LUMO+4 ($\delta-\delta \rightarrow \delta^*-\delta^*$), calculated at 459 nm. A similar $\delta \rightarrow \delta^*$ band was observed for **2** at 450 nm and calculated at 444 nm. The second absorption band for **1** at 460 nm can be assigned to the metal-to-ligand charge-transfer, which is a HOMO → LUMO+2 transition calculated at 466 nm. For **2**, a much more intense band at lower energy, 600 nm, was observed, and it corresponds to a HOMO → LUMO transition (metal $\delta-\delta$ to linker π^* orbital transition), which is calculated at 571 nm. This intense metal-to-ligand charge-transfer band is responsible for the dark-blue color of **2**. The Mo_2-to-sulfur electron hopping requires less energy than that for oxygen, and this explains why the −HN(S)C−C(S)NH− linked to **2** is more strongly coupled than the corresponding −HN(O)C−C(O)NH− bridged compound. A review of the available *dimer of dimers* suggests that, generally, for similar systems with closely related structures, the lower the energy for the metal-to-ligand charge transfer (MLCT) bands, the stronger the electronic coupling between the dimetal centers.[29] For example, compounds with uniquely strong electronic communication between dimetal centers, such as those linked by dioxolene dianions, are green colored and show even lower energy MLCT bands in the 1100 to 1200 nm region that have large extinction coefficients.[22] The studies on the analogous compounds having $[Mo_2(O_2CBu^t))_3]^+$ and $[W_2(O_2CBu^t)_3]^+$ units linked by oxalate or 3,6−dioxypyridazine show that the molybdenum compounds have MLCT absorption bands in UV−vis in the 400−500 nm range, whereas the more strongly coupled tungsten compounds exhibit MLCT bands at 700−800 nm.[28,30]

Scheme 4

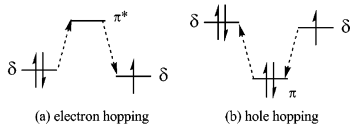

(27) It should be noted that the donation of electrons in the ä orbitals is unique to compounds with quadruply bonded units.

(28) Chisholm, M. H.; Clark, R. J. H.; Gallucci, J.; Hadad, C. M.; Patmore, N. J. *J. Am. Chem. Soc.* **2004**, *126*, 8303.

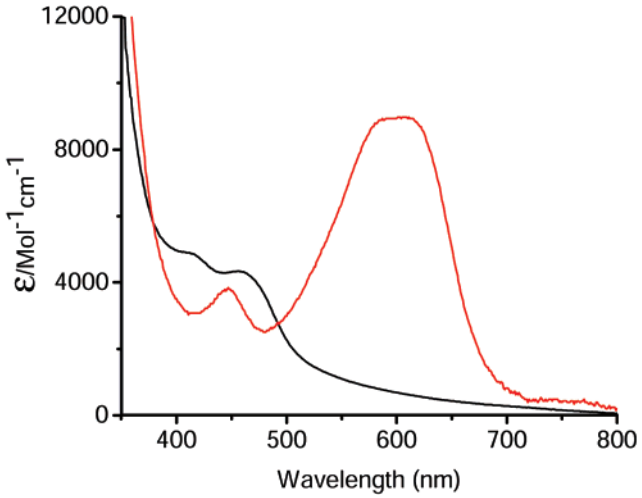

Figure 5. UV−vis spectra in a CH_2Cl_2 solution for **1** (black) and **2** (red).

Conclusions

The crystal structures of **1** and **2** that have *dimers of dimers* with dimolybdenum units linked by unsubstituted oxamidate and dithiooxamidate groups are isomorphous. The cores of the molecules are planar due to intramolecular hydrogen bonds in the bridging ligands. **2** reacts further with LiMe to form a lithium salt upon the removal of the remaining amine hydrogen atoms. The CVs of **1** and its sulfur analogue, **2**, show two reversible one-electron oxidation processes with potential separations ($\Delta E_{1/2}$) between the two oxidation processes of 204 and 407 mV, which correspond to K_c values of 2.8×10^3 and 7.6×10^6, respectively.

The distance between the $[Mo_2]$ units in **1** is similar (ca. 7 Å) to that linked by oxalate and diaryloxamidates (α form). However, the C−C bond in the oxalate-linked compound can rotate freely in solution, whereas the diaryloxamidate-linked compounds have two $[Mo_2]$ units that are essentially perpendicular to each other even in solution as a result of steric repulsions. The electronic coupling between the metal centers in these compounds is mainly determined by electrostatic interactions, and the different conformations of these species in solution has little affect on the electronic coupling (K_c on the order of 10^3).

By changing the oxygen donor atoms to sulfur atoms, the electronic coupling between the dimetal units changes substantially. The coupling in **2** is stronger than in **1** as evidenced by electrochemical data and DFT calculations on simplified models **1′** and **2′**. The latter suggest that the electronic structures are different and the energy of the linker's π^* orbital is much lower for **2′**, which in turn lowers the energy of the metal-to-ligand charge-transfer band. This is consistent with the electron transfer from the δ orbitals of the Mo_2 unit to the d orbitals of the sulfur atoms. The lower energy for the electron-hopping pathway explains the significant increase in electronic communication upon substitution of oxygen with sulfur atoms in a similar way as that observed in biological systems.[12]

(29) Chisholm, M. H.; Patmore, N. J. *Acc. Chem. Res.* **2007**, *40*, 19.
(30) Cayton, R. H.; Chisholm, M. H.; Huffman, J. C.; Lobkovsky, E. B. *J. Am. Chem. Soc.* **1991**, *113*, 8709.

Experimental Section

Materials and Methods. All of the reactions and manipulations were performed under a nitrogen atmosphere, using either a drybox or standard Schlenk line techniques. Solvents were purified under argon using a glass-contour solvent purification system or distilled over the corresponding drying agent under nitrogen. The starting material, $Mo_2(DAniF)_3(O_2CCH_3)$, was prepared following a reported procedure;[9a] other commercially available chemicals were used as received.

Analytical and Physical Measurements. Elemental analyses were performed by Robertson Microlit Laboratories, Madison, NJ. Electronic spectra were measured on a Shimadzu UV−2501PC spectrometer in a CH_2Cl_2 solution. ^{1}H NMR spectra were recorded on an Inova−300 NMR spectrometer with chemical shifts (δ ppm) referenced to residual $CHCl_3$ in $CDCl_3$. Cyclic voltammograms (CV) and differential pulse voltammograms were collected on a CH Instruments electrochemical analyzer with platinum working and auxiliary electrodes, a Ag/AgCl reference electrode, a scan rate (for CV) of 100 mV/s, and 0.10 M Bu_4NPF_6 (in CH_2Cl_2) as the electrolyte.

Preparation of $[Mo_2(DAniF)_3]_2$(Oxamidate), 1. To a solution of $Mo_2(DAniF)_3(OCCH_3)$ (508 mg, 0.500 mmol) and oxamide (22.0 mg, 0.250 mmol) in THF (15 mL), was added, slowly and with stirring, 0.5 M sodium methoxide (1.0 mL) in methanol. An orange solid formed in about 20 min. After 1 h, the solvent was evaporated under reduced pressure. The solid residue was extracted using CH_2Cl_2 (ca. 15 mL). The mixture was filtered using a Celite-packed frit, and the volume of the filtrate was reduced under a vacuum to about 5 mL. Then, 30 mL of isomeric hexanes was added, producing an orange precipitate. The solid was collected by filtration and dried under a vacuum. Yield: 325 mg (82%). Single crystals for X-ray analysis were obtained by diffusing hexanes into a dichloromethane solution of the orange product. ^{1}H NMR (δ, ppm in CD_2Cl_2): 10.27 (s, 2H, −N*H*), 8.50 (s, 2H, −NC*H*N−), 8.42 (s, 4H, −NC*H*N−), 6.60 ∼ 6.54 (m, 24H, aromatic C−*H*), 6.48 ∼ 6.43 (m, 8H, aromatic C−*H*), 6.41 ∼ 6.38 (d, 8H, aromatic C−*H*), 6.24 ∼ 6.21 (d, 8H, aromatic C−*H*), 3.70 (s, 12H, −OCH_3), 3.68 (s, 12H, −OCH_3), 3.66 (s, 6H, −OCH_3), 3.65 (s, 6H, −OCH_3). UV−vis, λ_{max} nm (ϵ, M^{-1}·mol^{-1}): 460 (2.0×10^3), 412 (1.1×10^3). Anal. Calcd for $C_{95}H_{98}Cl_6Mo_4N_{14}O_{14}$ (**1**·$3CH_2Cl_2$): C, 50.56; H, 4.38; N, 8.69. Found: C, 50.55; H, 4.67; N, 8.79.

Preparation of $[Mo_2(DAniF)_3]_2$(Dithiooxamidate), 2. To a solution of $Mo_2(DAniF)_3(OCCH_3)$ (406 mg, 0.40 mmol) and dithiooxamide (24.0 mg, 0.20 mmol) in THF (25 mL), was added, slowly and with stirring, 0.5 M sodium methoxide solution (0.8 mL) in CH_3OH. The color turned dark blue. The mixture was stirred at ambient temperature for 2 h. After removing the solvent under reduced pressure, the solid residue was extracted with CH_2Cl_2 (ca. 15 mL). The mixture was filtered using a Celite-packed frit, and the volume of the filtrate was reduced under a vacuum to ca. 5 mL. Then, 40 mL of ethanol was added, producing a blue precipitate, which was washed with ethanol (2×20 mL) and hexanes (20 mL). This solid was dried under a vacuum, dissolved again in 15 mL of CH_2Cl_2, and layered with hexanes. Blue crystals formed within 3 days. Yield: 345 mg (85%). ^{1}H NMR (δ, ppm in $CDCl_3$): 11.75 (s, 2H, −N*H*), 8.47 (s, 2H, −NC*H*N−), 8.35 (s, 4H, −NC*H*N−), 6.50 ∼ 6.65 (m, 40H, aromatic C−*H*), 6.18 (d, 8H, aromatic C−*H*), 3.73 (s, 12H, −OCH_3), 3.71 (s, 6H, −OCH_3), 3.69 (s, 12H, −OCH_3), 3.68 (s, 6H, −OCH_3). UV−vis, λ_{max} nm (ϵ, M^{-1}·mol^{-1}): 600 (8.0×10^3), 450 (1.1×10^3). Anal. Calcd for $C_{92}H_{92}Mo_4N_{14}O_{12}S_2$: C, 54.33; H, 4.56; N, 9.64. Found: C, 54.03; H, 4.62; N, 9.56.

Table 6. Crystallographic Data for **1** and **2**

	1·4CH_2Cl_2	**2**·4CH_2Cl_2
empirical formula	$C_{96}H_{100}Cl_8Mo_4N_{14}O_{14}$	$C_{96}H_{100}Cl_8Mo_4N_{14}O_{12}S_2$
fw	2341.26	2373.38
space group	$P\bar{1}$ (No. 2)	$P\bar{1}$ (No. 2)
a, Å	12.443(4)	12.386(5)
b, Å	14.608(5)	14.562(6)
c, Å	15.179(5)	15.500(6)
α, deg	72.118(5)	71.826(7)
β, deg	83.062(6)	83.923(7)
γ, deg	71.362(5)	71.386(6)
V, Å^3	2487.3(13)	2517.3(17)
Z	1	1
T, K	213	213
λ, Å	0.71073	0.71073
d_{calcd}, g/cm^3	1.563	1.566
μ, mm^{-1}	0.777	0.807
R1[a] (wR2[b])	0.0672(0.1424)	0.1148(0.1866)

[a] $R1 = ||F_o| - |F_c||/\sum|F_o|$. [b] $wR2 = [\sum[w(F_o^2 - F_c^2)^2]/\sum[w(F_o^2)^2]]^{1/2}$.

X−ray Structure Determinations. A single crystal of each compound was mounted and centered in the goniometer of a Bruker SMART 1000 CCD area detector diffractometer and cooled to −60 °C. Cell parameters were determined using the program *SMART*.[31] Data reduction and integration were performed with the software package *SAINT*,[32] and absorption corrections were applied using the program *SADABS*.[33] In all of the structures, the positions of the heavy atoms were found via direct methods using the program *SHELXTL*.[34] Subsequent cycles of least-square refinement followed by difference Fourier syntheses revealed the positions of the remaining non-hydrogen atoms. Disordered groups were divided into parts and refined with soft constraints. Hydrogen atoms were added in idealized positions. Non-hydrogen atoms were refined with anisotropic displacement parameters. Selected crystallographic data for **1**·4CH_2Cl_2 and **2**·4CH_2Cl_2 are in Table 6, and selected bond distances are in Table 1.

Computational Details. Molecular mechanics calculations were carried out using the software package *Cerius*^{2} by Accelrys[35] with the *Open Force Field* (OFF) program using the Universal Force Field. Density functional theory (DFT)[36] calculations were performed with the hybrid Becke's[37] three-parameter exchange functional and the Lee−Yang−Parr[38] nonlocal correlation functional (B3LYP) in the *Gaussian 03* program.[39] Double-ζ quality basis sets (D95)[40] were used on carbon, nitrogen, and hydrogen atoms as implemented in *Gaussian*. For oxygen and sulfur atoms, correlation-consistent double-ζ basis sets (CC−PVDZ)[41] were applied. A small ECP that represents the 1s2s2p3s3p3d core was used for the molybdenum atoms, along with its corresponding double-ζ basis set (LANL2DZ).[42] Time-dependent density functional (TD−DFT) calculations[43] were used for the assignment of the electronic spectra. All of the calculations were performed on either Origin 3800 64-processor SGI or Origin 2000 32-processor SGI supercomputers located at the Texas A&M supercomputing facility.

Acknowledgment. We thank the Robert A. Welch Foundation and Texas A&M University for financial support.

Supporting Information Available: X-ray crystallographic data for **1**·4CH_2Cl_2, **2**·4CH_2Cl_2, and **3**·2THF in standard CIF format, description of the synthesis of **3**, core structure of **3** (Figure S1), crystallographic data for **3** (Table S1), and selected bond distances and angles for **3** (Table S2). This material is available free of charge via the Internet at http://pubs.acs.org.

IC700932S

(31) *SMART*, version 5.05; Software for the CCD Detector System; Bruker Analytical X-ray System, Inc.: Madison, WI, 1998.
(32) *SAINT*, version 6.36A; Data Reduction Software; Bruker Analytical X−ray System, Inc.: Madison, WI, 2002.
(33) *SADABS*, version 2.03; Bruker/Siemens Area Detector Absorption and Other Corrections; Bruker Analytical X−ray System, Inc.: Madison, WI, 2002.
(34) *Sheldrick, G. M., SHELXTL*, version 6.12; Bruker Analytical X-ray Systems, Inc.: Madison, WI, 2000.
(35) *Cerius*^{2} *Forcefield-Based Simulations*, Accelrys Inc.: San Diego, CA, 2001.
(36) (a) Hohenberg, P.; Kohn, W. *Phys. Rev.* **1964**, *136*, B864. (b) Parr, R. G.; Yang, W. *Density-Functional Theory of Atoms and Molecules*; Oxford University Press: Oxford, U.K. 1989.
(37) (a) Becke, A. D. *Phys. Rev. A* **1988**, *38*, 3098. (b) Becke, A. D. *J. Chem. Phys.* **1993**, *98*, 1372. (c) Becke, A. D. *J. Chem. Phys.* **1993**, *98*, 5648.
(38) Lee, C. T.; Yang, W. T.; Parr, R. G. *Phys. Rev. B* **1998**, *37*, 785.
(39) Frisch, M. J.; Trucks, G. W.; Schlegel, H. B.; Scuseria, G. E.; Robb, M. A.; Cheeseman, J. R.; Montgomery, J. A., Jr.; Vreven, T.; Kudin, K. N.; Burant, J. C.; Millam, J. M.; Iyengar, S. S.; Tomasi, J.; Barone, V.; Mennucci, B.; Cossi, M.; Scalmani, G.; Rega, N.; Petersson, G. A.; Nakatsuji, H.; Hada, M.; Ehara, M.; Toyota, K.; Fukuda, R.; Hasegawa, J.; Ishida, M.; Nakajima, T.; Honda, Y.; Kitao, O.; Nakai, H.; Klene, M.; Li, X.; Knox, J. E.; Hratchian, H. P.; Cross, J. B.; Bakken, V.; Adamo, C.; Jaramillo, J.; Gomperts, R.; Stratmann, R. E.; Yazyev, O.; Austin, A. J.; Cammi, R.; Pomelli, C.; Ochterski, J. W.; Ayala, P. Y.; Morokuma, K.; Voth, G. A.; Salvador, P.; Dannenberg, J. J.; Zakrzewski, V. G.; Dapprich, S.; Daniels, A. D.; Strain, M. C.; Farkas, O.; Malick, D. K.; Rabuck, A. D.; Raghavachari, K.; Foresman, J. B.; Ortiz, J. V.; Cui, Q.; Baboul, A. G.; Clifford, S.; Cioslowski, J.; Stefanov, B. B.; Liu, G.; Liashenko, A.; Piskorz, P.; Komaromi, I.; Martin, R. L.; Fox, D. J.; Keith, T.; Al-Laham, M. A.; Peng, C. Y.; Nanayakkara, A.; Challacombe, M.; Gill, P. M. W.; Johnson, B.; Chen, W.; Wong, M. W.; Gonzalez, C.; Pople, J. A. *Gaussian 03*, revision C.02; Gaussian, Inc.: Wallingford, CT, 2004.
(40) (a) Dunning, T. H.; Hay, P. J. In *Modern Theoretical Chemistry. 3. Methods of Electronic Structure Theory*; Schaefer, H. F., III, Ed.; Plenum Publishing: New York, 1977; pp 1−28. (b) Woon, D. E.; Dunning, T. H. *J. Chem. Phys.* **1993**, *98*, 1358.
(41) (a) Dunning, T. H. *J. Chem. Phys.* **1989**, *90*, 1007. (b) Woon, D. E.; Dunning, T. H. *J. Chem. Phys.* **1993**, *98*, 1358. (c) Wilson, A. K.; Woon, D. E.; Peterson, K. A.; Dunning, T. H. *J. Chem. Phys.* **1999**, *110*, 7667.
(42) (a) Wadt, W. R.; Hay, P. J. *J. Chem. Phys.* **1985**, *82*, 284. (b) Hay, P. J.; Wadt, W. R. *J. Chem. Phys.* **1985**, *82*, 299.
(43) Casida, M. E.; Jamorski, C.; Casida, K. C.; Salahub, D. R. *J. Chem. Phys.* **1998**, *108*, 4439.